X SICEL 2021

Transición energética en la 4ta revolución industrial

Universidad Tecnológica de Pereira

UNIVERSIDAD NACIONAL DE COLOMBIA

XSICEL 2021

Transición energética en la 4ta revolución industrial

Small-Signal Stability and Sensitivity Analysis for Grid Following Converters

Authors:
Simon Sepulveda Garcia
Alejandro Garces Ruiz

Institution:
Universidad Tecnologica de Pereira

Contents

I. Introduction

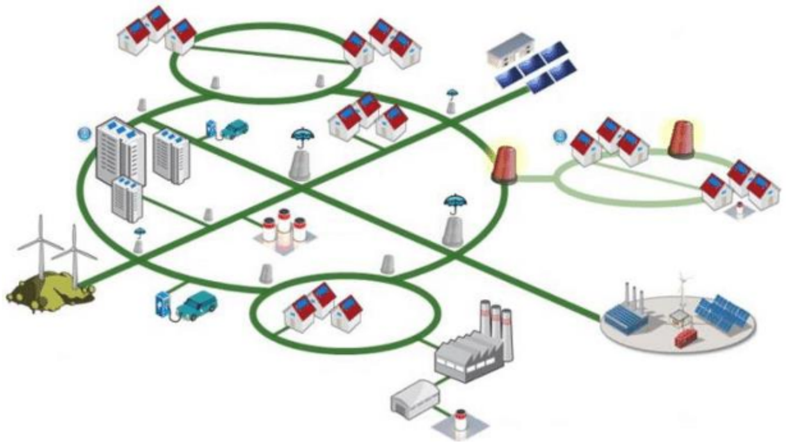

Figure 1. Active distribution network

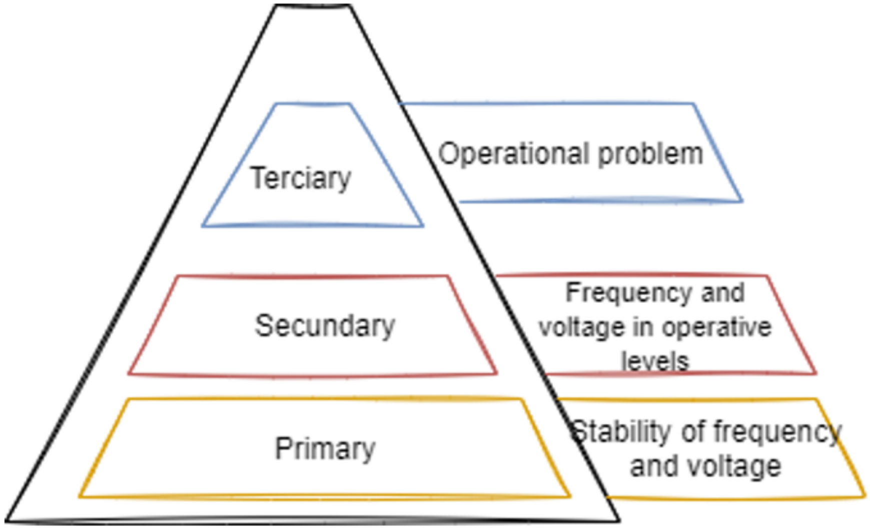

Figure 2. Schematic diagram of the hierarchical control in active distribution systems

II. Theoretical aspects

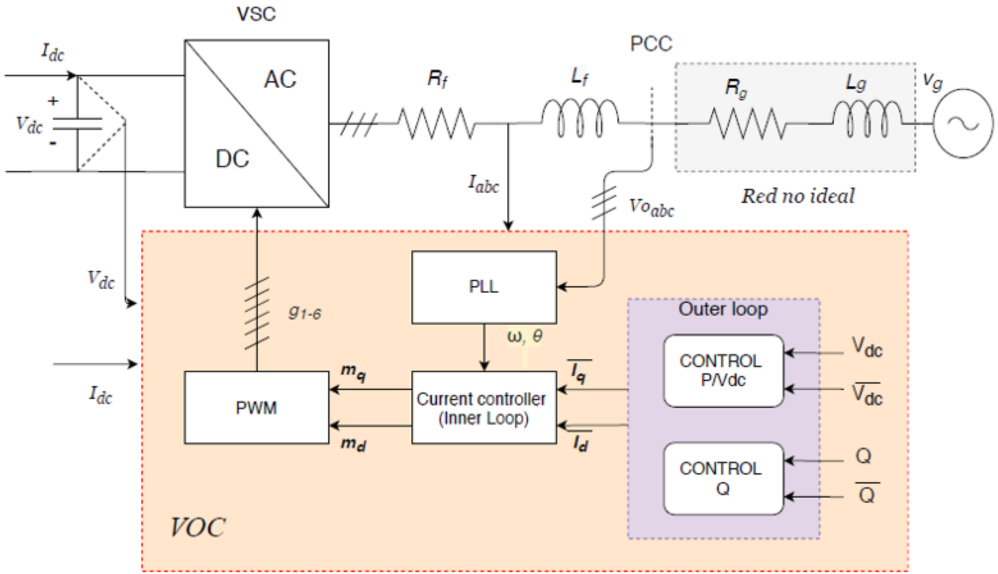

Figure 3. Voltage source converter (VSC) with vector-oriented control (VOC)

II. Theoretical aspects

$$x_a + x_b + x_c = 0$$

$$\begin{pmatrix} x_\alpha \\ x_\beta \end{pmatrix} = k \begin{pmatrix} 1 & -\frac{1}{2} & -\frac{1}{2} \\ 0 & -\frac{\sqrt{3}}{2} & \frac{\sqrt{3}}{2} \end{pmatrix} \begin{pmatrix} x_a \\ x_b \\ x_c \end{pmatrix}$$

$$p_{\alpha\beta 0} = [V_{\alpha\beta 0}]^\top [I_{\alpha\beta 0}]$$

$$p_{\alpha\beta 0} = [V_{abc}]^\top [TC]^\top [TC][I_{abc}]$$

$$p_{\alpha\beta 0} = \frac{2}{3}[V_{abc}][I_{abc}]$$

$$p_{\alpha\beta 0} = \frac{2}{3} p_{abc}$$

SEC. 1 Clark transformation

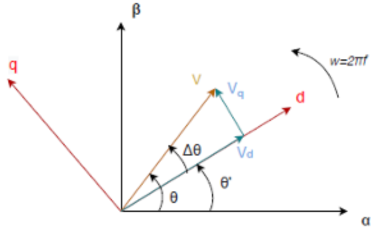

$$\begin{pmatrix} x_d \\ x_q \end{pmatrix} = \begin{pmatrix} \cos(\theta') & \sin(\theta') \\ -\sin(\theta') & \cos(\theta') \end{pmatrix} \begin{pmatrix} x_\alpha \\ x_\beta \end{pmatrix}$$

SEC. 2 Park transformation

$$p_{\alpha\beta 0} = p_{odq}$$

$$p_{abc} = \frac{3}{2} p_{odq}$$

$$p = \frac{3}{2}(v_d i_d + v_q i_q) \qquad q = \frac{3}{2}(v_q i_d - v_d i_q)$$

SEC. 3 Active and reactive power in the dq frame

Note: SEC mean set of equations

II. Theoretical aspects

The current dynamics of the system on the AC side can be obtained by applying kirchoff's second law

$$(L_f + L_g)\frac{di_d}{dt} = -w(L_g + L_f)i_q - (R_g + R_f)i_d - V_g^d + V_d^s$$

$$(L_f + L_g)\frac{di_q}{dt} = w(L_f + L_g)i_d - (R_f + R_g)i_q - V_q^g + V_q^s$$

it is also possible to obtain the voltage dynamics of the DC side of the converter through the power balance.

$$C\frac{dV_{dc}}{dt} = I_{dc} - \frac{3V_d^s i_d}{2V_{dc}}$$

SEC. 4 Dynamics of the grid

II. Theoretical aspects

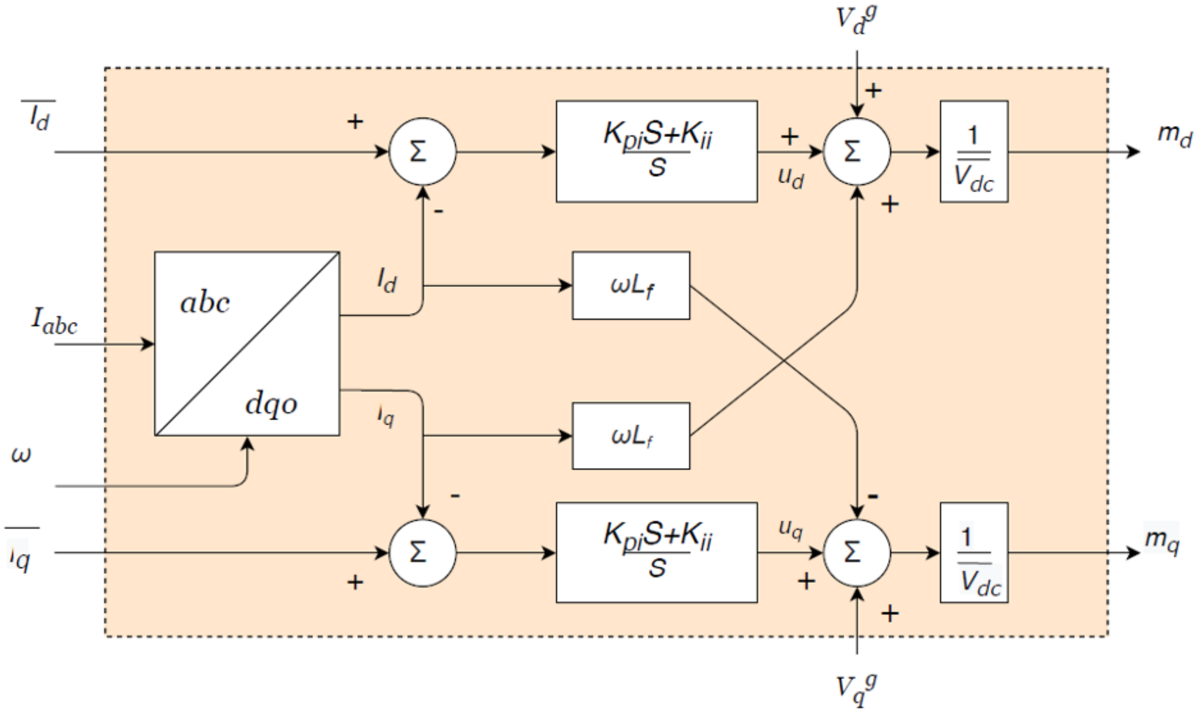

Figure 3. Inner Loop

II. Theoretical aspects

The inner loop can be described mathematically by adding a couple of auxiliary variables $\gamma_{d/q}$

$$\frac{d\gamma_d}{dt} = \bar{i}_d - i_d$$

$$\frac{d\gamma_q}{dt} = \bar{i}_q - i_q$$

$$V_d^s = V_d^g + R_g i_d - R_f \frac{L_g}{L_f} i_d + \frac{L_f + L_g}{L_f}(wL_f i_q + k_{pi}(\bar{i}_d - i_d) + k_{ii}\gamma_d)$$

$$V_q^s = V_q^g + R_g i_q - R_f \frac{L_g}{L_f} i_q + \frac{L_f + L_g}{L_f}(-wL_f i_d + k_{pi}(\bar{i}_q - i_q) + k_{ii}\gamma_q)$$

SEC. 5 Mathematical description of the Inner loop

II. Theoretical aspects

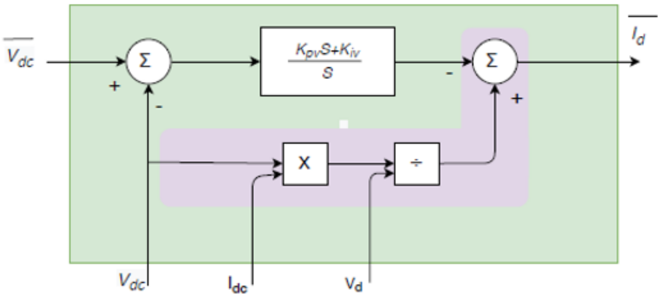

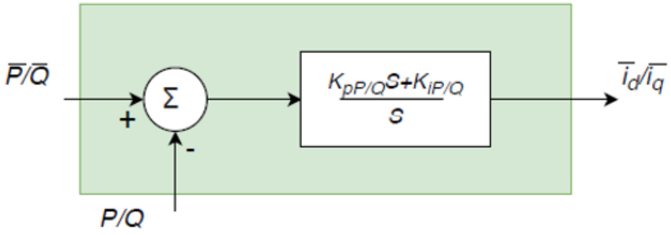

Figure 4. Outer Loop

II. Theoretical aspects

The outer loop can be described mathematically by adding a couple of auxiliary variables $\gamma_{v/q}$.

$$\frac{d\gamma_v}{dt} = \bar{V}_{dc} - V_{dc}$$

$$\bar{I}_d = k_{pv}(\bar{V}_{dc} - V_{dc}) + k_{iv}\gamma_v$$

$$\frac{d\gamma_q}{dt} = \bar{Q} - Q$$

$$\bar{I}_q = K_{pq}(\bar{Q} - Q) + K_{iQ}\gamma_Q$$

SEC. 6 Mathematical description of the Inner loop

II. Theoretical aspects

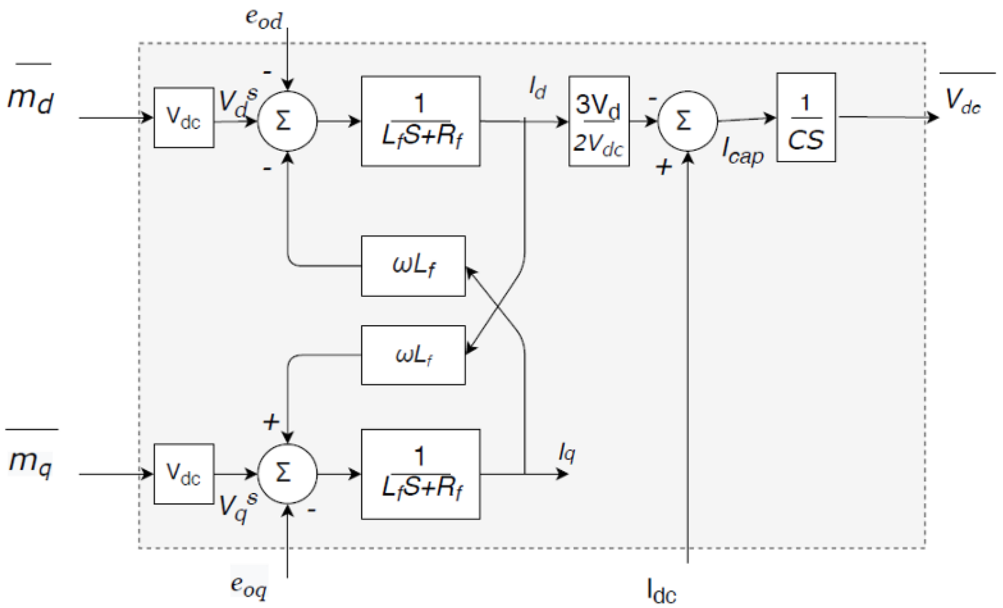

Figure 4. Dynamic model of the VSC

II. Theoretical aspects

The state-space model of the converter can be rewritten as

$$\dot{x} = f(x, y, u)$$
$$y = g(x, u)$$

Where x represents the state variables, y represents the control variables and u represents the input variables.

$$\Delta\dot{x} = A\Delta x + B\Delta u$$

Where:

$$A = J(X_0) = \frac{\partial f}{\partial x} + \frac{\partial f}{\partial g}\frac{\partial g}{\partial x}|_{x=x_0}$$
$$B = \frac{\partial f}{\partial u} + \frac{\partial f}{\partial g}\frac{\partial g}{\partial u}|_{u=u_0}$$

II. Theoretical aspects

The state, control and input variables of the VSC are respectively:

$x = [i_d, i_q, V_{dc}, \gamma_d, \gamma_q, \gamma_v]^T \quad u = [V_d^g, V_{dc}, I_{dc}, i_q*]^T \quad y = [V_d^s, V_q^s]^T$

Taking this into account, it is possible to obtain the operating point (or initial condition) of the system assuming that it is operating at steady state

Variable	Initial condition
i_{do}	$\frac{-v_g^d + \sqrt{(v_d^g)^2 + \frac{8 v_{dc} I_{dc} (R_g + R_f)}{3}}}{2(R_f + R_g)}$
i_{qo}	$i_q = 0$
v_{dco}	V_{dc}
γ_{do}	$\frac{i_{d0} R_f}{k_{ii}}$
γ_{qo}	0
γ_{vo}	$-\frac{i_{d0}}{k_{iv}}$

Table 1. Initial conditions

II. Theoretical aspects

Where the state matrix is described in

$$A = \begin{pmatrix} \frac{-R_s - k_{pi}}{L_f} & 0 & \frac{k_{pi}k_{pv}}{L_f} & \frac{k_{ii}}{L_f} & 0 & -\frac{k_{pi}k_{iv}}{L_f} \\ 0 & \frac{-R_s - k_{pi}}{L_f} & 0 & 0 & \frac{k_{ii}}{L_f} & 0 \\ J_{31} & J_{32} & J_{33} & J_{34} & 0 & J_{36} \\ -1 & 0 & k_{pv} & 0 & 0 & -k_{iv} \\ 0 & -1 & 0 & 0 & 0 & 0 \\ 0 & 0 & -1 & 0 & 0 & 0 \end{pmatrix}$$

$$J_{31} = -\frac{3(V_d^g + (R_f + R_g)i_{d0} - R_f \frac{L_g}{L_f} i_{do} - \frac{L_f + L_g}{L_f} k_{pi} i_{do})}{2CV_{dc}}$$

$$J_{32} = -\frac{3(i_{do} w_o L_f)}{2CV_{dc}} \frac{L_f + L_g}{L_f}$$

$$J_{33} = \frac{3i_{do}(V_d^g + R_f i_{do} - \frac{L_f + L_g}{L_f} k_{pi} k_{pv} V_{dc})}{2CV_{dc}^2}$$

$$J_{34} = -\frac{3(i_{do} k_{ii})}{2CV_{dc}} \frac{L_f + L_g}{L_f}$$

$$J_{36} = \frac{3 i_{do} k_{pi} k_{iv}}{2CV_{dc}} \frac{L_f + L_g}{L_f}$$

SEC. 7 State matrix of the VSC.

II. Theoretical aspects

The sensitive analysis aims to determine the influence of each element of the state matrix in the system's eigenvalues

$$p_i^{km} = \frac{\partial \lambda_i}{\partial a_{km}} = \varphi_i^k \phi_i^m$$

It is difficult to visualize the results in a tensor, therefore, it is more useful to analyze the influence of a specific parameter of the system in the position of the eigenvalues. Thus, by applying chain of rule to the above equation

$$p_i^x = \sum_{k=1}^{n} \sum_{m=1}^{n} \frac{\partial \lambda_i}{\partial a_{km}} \frac{\partial a_{km}}{\partial x}$$

III. Numerical results

From the state matrix it is possible to obtain the eigenvalues of the system, which are as follows.

$$\lambda = \begin{pmatrix} -112.179 + 436.585j & -112.179 - 436.585j \\ -195.482 + 135.993j & -195.482 - 135.993j \\ -267.000 + 266.120j & -267.000 - 266.120j \end{pmatrix}$$

from the same state matrix, it is possible to obtain the real part of the participation factors, as illustrated in the following table

Participation factor	L_f	C
p_1	3796.68	-4171.90
p_2	3796.68	-4171.90
p_3	1057.86	2245.72
p_4	1057.86	2245.72
p_5	4854.54	-1.14×10^{-27}
p_6	4854.54	-1.14×10^{-27}

Table 2. Participation factors (real part) system parameters.

III. Numerical results

However, it is important to know the influence on the imaginary part, because it directly influences the damping factors.

$$r_D = -\frac{\alpha}{\sqrt{\alpha^2 + \beta^2}} 100\%$$

Participation factor	L_f	C
p_1	-690.37	-96230.6
p_2	690.37	96230.6
p_3	-777.58	22583.16
p_4	777.585	-22583.16
p_5	16.01	3.44×10^{-27}
p_6	-16.01	-3.44×10^{-27}

Table 3. Participation factors (imaginary part) system parameters.

Factor	L_f	L_g
$p_{1,2}$	3947.41 ± 288.29	475.8 ± 55.07
$p_{3,4}$	1180.67 ± 686.03	161.97 ± 84.83
$p_{5,6}$	4856.19 ± 509.26	$-3.270 \times 10^{-30} \pm 6.66 \times 10^{-31}$

Table 4. Participation factors of the non ideal grid.

III. Numerical results

The corresponding participation factors of the parameters of the PI type controllers are as follows

Participation factor	k_{pi}	k_{pv}	k_{ii}	k_{iv}
p_1	-6.83	-91.424	-0.0035	0.371
p_2	-6.83	-91.424	-0.0035	0.371
p_3	-3.65	56.75	0.0035	-0.37
p_4	-3.65	56.75	0.0035	-0.37
p_5	-9.09	3.92×10^{-30}	-1.911×10^{-19}	-3.49×10^{-32}
p_6	-9.09	3.92×10^{-30}	-1.911×10^{-19}	-3.49×10^{-32}

Factor	k_{pi}	k_{pv}	k_{ii}	k_{iv}
p_1	0.26	149.7	0.018	0.115
p_2	-0.26	-149.7	-0.018	-0.115
p_3	-3.14	-72.74	0.013	0.113
p_4	3.14	72.74	-0.013	-0.113
p_5	-8.92	3.86×10^{-30}	0.033	-2.20×10^{-32}
p_6	8.92	-3.86×10^{-30}	-0.033	2.20×10^{-32}

Table 5 and 6. Participation factors of the control parameters.

III. Numerical results

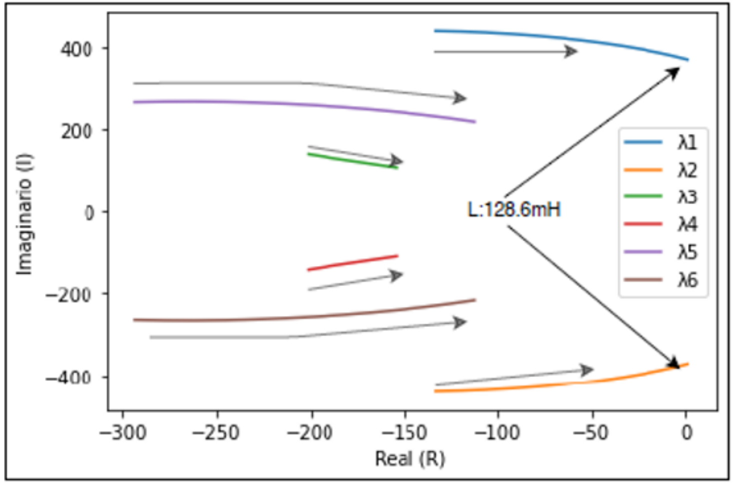

Figure 5. Bifurcation of the system for L [50 – 150]mH

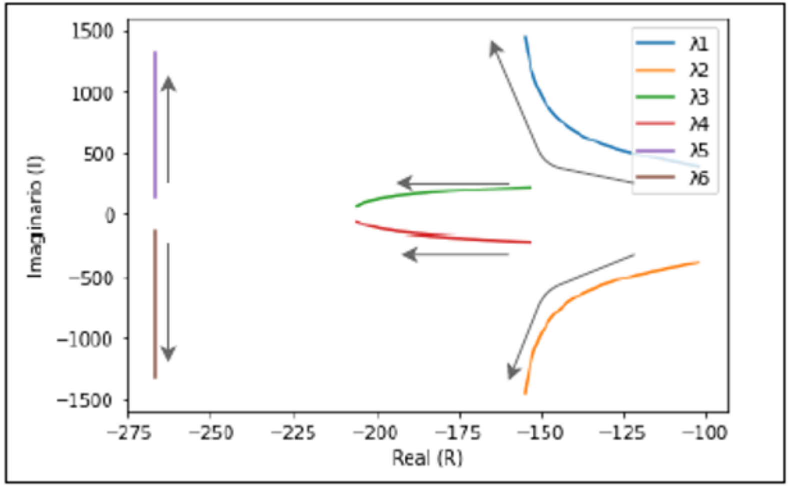

Figure 5. Bifurcation of the system for kii [5 - 100] $\times 10^3$

IV. CONCLUSIONS

- In this paper, a sensitivity analysis is used to determine numerically how system parameters and controller constants influence the stability of a VSC operating as a grid feeder, Demonstrating its usefulness in determining variables that can cause instability and those that are desirable to control in order to improve it.
- An increase in the proportional action increases the stability margins of all the eigenvalues, which is useful since it can be coordinated with a high inductance (or capacitance) value for filtering, which decreases these margins.
- A high value for the integral action is desired to ensure zero steady state error, however, as can be seen from the analysis, a high value results in a significant decrease in the damping ratios
- The non-ideal network is a parameter that depends on the connection point; therefore, its impedance varies. It must be taken into account because, as demonstrated, it affects the stability margins and also worsens the sensitivity of the system.